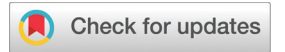
# **Green Chemistry**



PAPER View Article Online
View Journal | View Issue



**Cite this:** *Green Chem.*, 2020, **22**, 5395

# Electrohydrodimerization of biomass-derived furfural generates a jet fuel precursor†

Xiao Shang, Yang Yang 📵 and Yujie Sun 🔘 \*

Despite the increasing interest in upgrading biomass-derived molecules to value-added products, the electrochemical conversion of biomass platform chemicals to highly valuable biofuels, such as jet fuel, has not yet received wide attention. Herein, we report a catalyst-free electrochemical route for the production of a jet fuel precursor, hydrofuroin, from the electrohydrodimerization of furfural, which can be readily derived from lignocellulose and already has an industrial production of 300 000 tons per year. Detailed electrochemical studies using carbon and copper electrodes at various pH values enabled us to probe the reduction mechanism of furfural and obtain the kinetic details, such as the diffusion constant and electron transfer rate. Preparative electrolysis in a batch electrolyzer achieved a high yield of hydrofuroin (94%) with an excellent faradaic efficiency of 93%. Finally, a flow electrolyzer was employed to demonstrate the great promise of large-scale production of hydrofuroin from the electrohydrodimerization of furfural.

Received 20th May 2020, Accepted 13th July 2020 DOI: 10.1039/d0gc01720e rsc.li/greenchem

#### Introduction

The extensive utilization of fossil resources driven by increasing global energy demand has not only caused the rapid depletion of non-renewable carbons but also released enormous amounts of greenhouse gases, primarily CO2, which will lead to detrimental climate changes in the long term. Hence, it is urgent to explore alternative carbon sources whose utilization will not alter the carbon balance of our current ecosystem. Within this context, biomass is the only viable candidate of sustainable non-fossil carbon sources because of its green nature and global abundance. At the end of the utilization of biomass-derived products, the released CO2 will be used to produce new biomass via photosynthesis, resulting in an overall carbon-neutral cycle. In order to transform natural biomass into marketable products, a large amount of effort has been devoted to developing effective biomass valorization techniques. Among the many bioproducts, biofuels represent an appealing target as our transportation sector heavily relies on fossil fuels and is one of the largest contributors towards CO<sub>2</sub> emission.<sup>2,3</sup> In fact, the applicability of biofuels has been manifested by the successful adoption of first-generation bioethanol and biodiesel in the current infrastructure. In order to expand the scope of biofuel candidates, jet fuel has

become an attractive target due to its high value but remained much less pursued in biomass valorization.

After the US Department of Energy released a list of top biomass-derived platform chemicals, furanics, such as furfural<sup>4</sup> and 5-hydroxymethylfurfural (HMF) obtained from lignocellulose, have attracted increasing attention because they can be upgraded to a variety of industrially important products, ranging from polymer precursors, fine chemicals, and solvents to fuels and fuel additives. 5-8 Conversion of furanics to fuel additives such as 2-methylfuran9 and 2,5-dimethylfuran<sup>8,10</sup> proceeds via dehydration, 11 hydrogenation, 12 hydrodeoxygenation, 13 or decarbonylation. 14 However, these lowcarbon-number alkanes with high volatility and low energy density are not applicable for direct drop-in fuels. A more attractive option for the conversion of furanics is to elongate their carbon chains to obtain precursors followed by hydrodeoxygenation to generate alkanes with satisfactory qualities (e.g., molecular weight and volatility) for transportation fuels. Many C-C bond-forming strategies to produce fuel precursors have been developed, including aldol condensation, hydroxyalkylation, ketonization, and oligomerization.<sup>7</sup>

One appealing strategy for the valorization of furanics is the C–C coupling reaction. For example, Ru-doped ZnIn<sub>2</sub>S<sub>4</sub> has been recently reported to catalyse the C–C coupling of 2-methylfuran under visible light irradiation to produce a mixture of diesel precursors;<sup>15</sup> however, the mediocre reaction rate and quantum yield render this photocatalytic approach challenging for large-scale applications. Furthermore, 2-methylfuran is a downstream product of furfural. It would be more cost effective to directly employ furfural, which has an

Department of Chemistry, University of Cincinnati, Cincinnati, OH 45221, USA. E-mail: vuiie.sun@uc.edu

 $<sup>\</sup>dagger\,\mathrm{Electronic}$  supplementary information (ESI) available. See DOI: 10.1039/d0gc01720e

Paper Green Chemistry

industrial production of 300 000 tons per year,8 to produce biofuel precursors of even higher value, such as jet fuel. The homocoupling of furfural to produce C<sub>10</sub> furoin or hydrofuroin has been previously investigated using N-heterocyclic carbenes (NHC) as catalysts in ionic liquids. 16,17 Although these results are promising, the use of expensive ionic liquids makes this approach less attractive for large-scale employment.

Similar to the success of photochemistry in organic synthesis during the last decade, electrochemistry has gained renaissance for a diverse array of organic reactions, 18 including the upgrading of biomass-derived furanics to value-added products. 19,20 The plethora of electrochemical parameters and the green nature of electricity originating from renewable resources such as the sun and wind make organic electrochemistry very attractive for biomass valorization. Through either oxidation or reduction, a large number of commodity chemicals which were originally obtained via thermocatalysis under harsh conditions have been produced electrochemically under benign conditions. 21-24 For instance, our group has developed several electrocatalytic systems for the oxidation of HMF to yield 2,5-furandicarboxylic acid (FDCA), which is a green polymer precursor and a replacement for terephthalic acid. 25-28 However, most reported electrochemical studies have focused on unimolecular transformation<sup>29</sup> and very few studies have been devoted to exploring electrochemical C-C bond formation in furanics, even though the electroreductive coupling of carbonyls is a well-established reaction in organic electrochemistry.30

Herein, we report a catalyst-free electrohydrodimerization of furfural to hydrofuroin, which is a jet fuel precursor (Scheme 1). A low-cost and eco-friendly carbon electrode was able to perform competently the electrolysis of furfural coupling in an alkaline electrolyte (0.1 M KOH), achieving a hydrofuroin yield of 94% with a faradaic efficiency of 93% in a batch electrolyzer. Furthermore, we demonstrate that a flow electrolyzer can also be utilized to realize an equally high yield and faradaic efficiency but with a much faster production rate, highlighting the promise of electrochemical furfural coupling in a large-scale application. Control experiments performed under various conditions aid our mechanistic understanding in the



Scheme 1 Electrohydrodimerization of biomass-derived furfural in aqueous electrolytes to generate hydrofuroin which can be further converted to produce a jet fuel candidate of the linear alkane C<sub>10</sub>H<sub>22</sub>.

formation of hydrofuroin from furfural coupling versus the formation of furfural alcohol from its hydrogenation, which enables the selective production of either hydrofuroin or furfural alcohol.

### Experimental

Furfural, furfural alcohol, potassium hydroxide, concentrated sulfuric acid, dipotassium phosphate, potassium phosphate monobasic, ammonium acetate, nickel chloride, ammonium chloride, Ni foam, carbon paper, Cu foam and the anion exchange membrane (Fumasep FAA-3-PK-130) were purchased from commercial vendors and used as received.

Electrochemical experiments were performed using a CHI 760E electrochemical workstation. A piece of carbon paper  $(1.0 \text{ cm} \times 1.0 \text{ cm})$  was employed as the working electrode, a carbon rod as the counter electrode, and a Ag/AgCl (saturated KCl aqueous electrolyte) electrode as the reference electrode. The electroreduction performance of furfural was also studied using different working electrodes, such as Cu foam (1.0 cm × 1.0 cm). All electrochemical experiments were conducted in a two-compartment cell composed of anode and cathode compartments, which were separated by an anion exchange membrane. The deaerated electrolyte containing furfural was protected under N2. The rotating disk electrode (RDE) experiments were performed using an MSR Electrode Rotator (Pine Research Instrumentation).

The products were quantified via high-performance liquid chromatography (HPLC). To analyze the products of electrochemical reduction of furfural quantitatively and to calculate the corresponding faradaic efficiencies, 10 µL of the electrolyte solution during chronoamperometry was collected and diluted with 1.99 mL of water, which was analyzed by HPLC using an Agilent 1260LC instrument at room temperature. The HPLC instrument was equipped with an ultravioletvisible detector set at 230 nm and a C18 column. The eluent solvent was a mixture of 5 mM ammonium formate aqueous solution (80%) and methanol (20%). The flow rate was 0.5 mL  $min^{-1}$ .

The conversion (%) of furfural and the yield (%) of the electroreduction products were calculated based on the following two equations:

$$\begin{split} \text{Conversion}(\%) &= \frac{\text{mole of substrate consumed}}{\text{mole of initial substrate}} \times 100\% \\ &\text{Yield}(\%) = \frac{\text{mole of product formed}}{\text{mole of initial substrate}} \times 100\% \end{split}$$

The faradaic efficiency (FE) of the product was calculated based on the following equation:

$$\mathrm{FE}(\%) = \frac{\mathrm{mole\,of\,product\,formed}}{\mathrm{total\,charge\,passed}/(n \times F)} \times 100\%$$

where n is the number of electrons transferred for each product formation and F is the Faraday constant (96 485 C  $\text{mol}^{-1}$ ).

Green Chemistry Paper

#### Preparation of Ni/NF

The Ni/NF electrode was prepared according to previous literature with modifications.  $^{27}$  Typically, electrodeposition was performed in a standard three-electrode configuration at room temperature. Ni foam (5.0 cm  $\times$  1.0 cm) was used as the working electrode, with a carbon rod and a Ag/AgCl (saturated KCl) electrode as the counter and reference electrodes, respectively. The electrolyte was 2.0 M NH<sub>4</sub>Cl and 0.1 M NiCl<sub>2</sub>. Chronoamperometry was conducted at -500~mA for 300 s.

#### Electrochemical reduction of furfural in a flow electrolyzer

In a typical process, 10 pieces of carbon paper (1.0 cm  $\times$  5.0 cm) were fixed into the cathode compartment and three pieces of Ni/NF (1.0 cm  $\times$  5.0 cm) were fixed into the anode compartment. Subsequently, 10 mL of 0.1 M KOH electrolyte and 10 mL of 0.1 M KOH containing 10 mM furfural were pumped using a PHD Ultra instrument into the anode and cathode compartments, respectively, with a flow rate of 0.5 mL min $^{-1}$ . The flow electrolyzer was controlled by a Gamary 1000 Interface electrochemical workstation. Periodically, 5 mL of the electrolyte outlet from the cathode chamber was collected and extracted with CHCl $_3$  several times prior to HPLC and NMR analysis.

#### Results and discussion

Since the H<sub>2</sub> evolution reaction (HER) is the primary competing reaction for any reductive transformations in aqueous electrolytes, it is of critical importance to choose electrodes that exhibit poor HER activity for furfural coupling in order to achieve an appreciable faradaic efficiency. Previous studies for the reductive transformation of furfural were usually conducted in strongly acidic electrolytes (*e.g.*, 0.5 M H<sub>2</sub>SO<sub>4</sub>), wherein furfural alcohol and 2-methylfuran were the target products.<sup>19,31</sup> Even though electrodes of C, Fe, and Al were found to produce hydrofuroin with decent selectivity, the corresponding faradaic efficiencies were rather poor at low pH.

Fig. 1a–c present the cyclic voltammograms of a carbon paper electrode obtained in 0.5 M  $\rm H_2SO_4$  (pH 0), 0.1 M phosphate buffer (pH 7), and 0.1 M KOH (pH 13), respectively. It is apparent that in 0.5 M  $\rm H_2SO_4$ , the cathodic current took off, presumably due to the HER, at a less negative potential (–0.9 V  $\nu s$ . Ag/AgCl) than those in 0.1 M phosphate buffer (–1.2 V  $\nu s$ . Ag/AgCl) and 0.1 M KOH (–1.3 V  $\nu s$ . Ag/AgCl). Upon the addition of 10 mM furfural, a much rapid cathodic current rise was observed for each condition with an anodically shifted onset potential, implying the favourable reduction of furfural relative to the HER. If Cu foam was utilized as the working electrode, much smaller onset shifts were obtained (ESI Fig. 1†). Moreover, the current rises were also less apparent at more negative potentials.

Controlled potential electrolysis was subsequently conducted in these three electrolytes with 10 mM furfural and the products were identified and quantified via <sup>1</sup>H NMR (ESI Fig. 2 and 3†). In order to distinguish the performance differ-

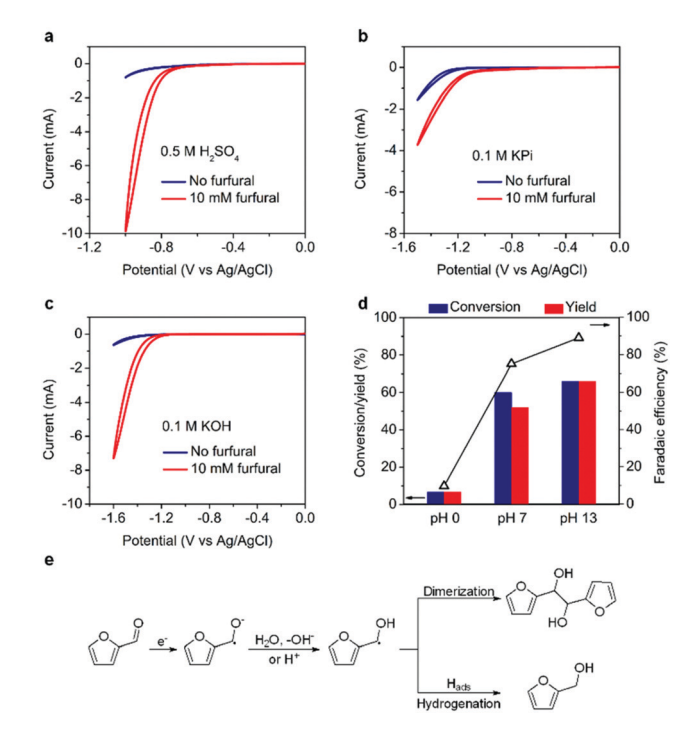


Fig. 1 Cyclic voltammograms of a carbon paper electrode obtained in (a) 0.5 M H<sub>2</sub>SO<sub>4</sub>, (b) 0.1 M phosphate buffer at pH 7, and (c) 0.1 M KOH in the absence (black) and presence (red) of 10 mM furfural (scan rate = 50 mV s<sup>-1</sup>). (d) Furfural conversion, hydrofuroin yield, and faradaic efficiency for partial electrolysis conducted at -0.9 V vs. Ag/AgCl at pH 0 and -1.4 V vs. Ag/AgCl at pH 7 and 13. The passed charge of each electrolysis was fixed at 10 C, while the complete conversion of 10 mM furfural to hydrofuroin required  $\sim\!\!14$  C. (e) Reductive conversion pathways of furfural to yield hydrofuroin or furfural alcohol.

ences at different pH values, the passed charge of each electrolysis was fixed at 10 C while the theoretical charge was ~14 C for the complete conversion of furfural to hydrofuroin. In 0.5 M H<sub>2</sub>SO<sub>4</sub>, the applied potential on carbon paper was set at -0.9 V vs. Ag/AgCl and a substantial current increase was obtained upon furfural addition while the background HER current was quite small (Fig. 1a). However, after the passage of 10 C, the conversion of furfural was only 7% even though the selectivity was nearly 100% for the formation of hydrofuroin, whose yield was 7% (Fig. 1d). The calculated faradaic efficiency was rather poor, 10%, implying that the HER was the dominant reaction on carbon paper in a strongly acidic electrolyte. In contrast, much improved performance was obtained at higher pH values. At an applied potential of -1.4 V vs. Ag/AgCl, the carbon paper electrode exhibited decent performance towards furfural coupling to hydrofuroin at both pH 7 and pH 13 (Fig. 1d), achieving a furfural conversion of 60% and 66%, respectively. The hydrofuroin yields were 52% (pH 7) and 66% (pH 13) with faradaic efficiencies of 75% and 89%, respectively. Although a decent furfural conversion was realized at pH 7, an appreciable amount of furfural alcohol was also detected (ESI Fig. 2†) and hence resulted in a relatively lower selectivity (86%) towards the formation of hydrofuroin than at pH 13 (nearly 100%). Given the negligible electroPaper Green Chemistry

chemical resistance differences among the electrolytes of different pH values (ESI Fig. 4†), these results unambiguously demonstrated that alkaline conditions significantly suppressed other competing reactions (e.g., HER and hydrogenation) while they favored the electrohydrodimerization of furfural to hydrofuroin.

In sharp contrast, if copper foam was utilized as the cathode for furfural electrolysis, the final products were quite distinct from those obtained on carbon paper (ESI Fig. 3 and 5†). At pH 0, furfural alcohol was detected as the major product, in agreement with the fact that copper is a better hydrogenation electrode than carbon. 32,33 Although the furfural conversion, hydrofuroin yield, and its faradaic efficiency were also improved at higher pH values, the highest hydrofuroin yield was only 60% at pH 13 with a large amount of furfural alcohol co-produced.

The drastic difference between carbon and copper electrodes in electrolytes of varying pH values prompted us to further probe the reduction mechanism of furfural. Cyclic voltammograms (CVs) of furfural using a carbon paper electrode were obtained at scan rates faster than 1 V s<sup>-1</sup> in acetonitrile, a proton-free environment. As shown in ESI Fig. 6a,† a quasireversible redox feature was observed, which was in sharp contrast to a completely irreversible process in 0.1 M KOH (ESI Fig. 6b†). These results demonstrated that upon one-electron reduction, the in situ-formed furfural radical anion could be oxidized back to the original state in a proton-free electrolyte if a fast scan rate was employed. However, in aqueous media, protonation at the oxygen atom would immediately follow the formation of the furfural radical anion and result in the generation of a neutral radical. Subsequently, two possible pathways will be followed as displayed in Fig. 1e: (i) a second proton-coupled electron transfer (hydrogenation) to yield furfural alcohol or (ii) radical dimerization to produce hydrofuroin.31 The preference of these two routes is largely determined by the relative potential required for the formation of the adsorbed hydrogen (Hads) on the cathode. Since copper is more active in catalysing H<sub>2</sub> evolution than carbon, it is known that H<sub>ads</sub> will form on copper at a much less negative potential than on carbon, which is in agreement with the smaller onset potentials of the HER on copper regardless of the electrolyte pH. Therefore, once the furfural radical is formed on copper, a subsequent hydrogenation step will take place and furfural alcohol will more likely form. However, there is no sufficient Hads generated on carbon at the potential for the formation of the furfural radical at pH 13; hence dimerization is the dominant route. Overall, high electrolyte pH and low Hads formation will favour the production of hydrofuroin from furfural coupling, whereas low electrolyte pH and efficient Hads generation on the working electrode facilitate the formation of furfural alcohol.

Since the second dimerization step was a non-electrochemical process,<sup>34</sup> the first electrochemical reduction step of furfural was further investigated on glassy carbon electrodes in order to gain more kinetic insights. Fig. 2a presents the CVs of furfural obtained at different concentrations. The irreversible

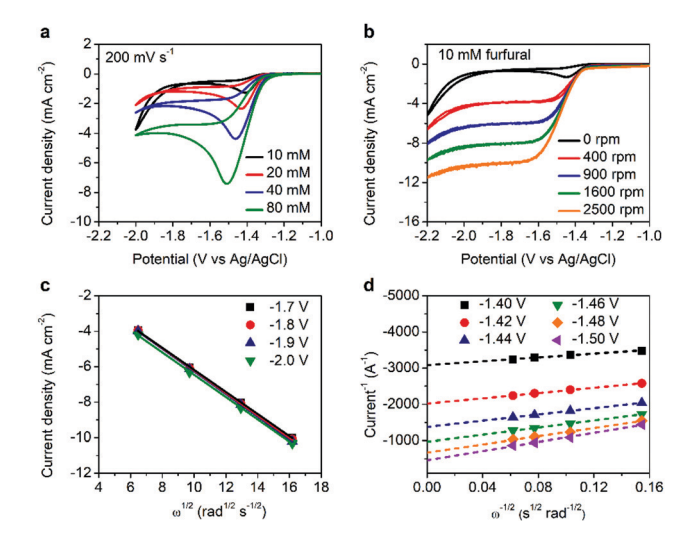


Fig. 2 (a) Cyclic voltammograms of furfural reduction with different substrate concentrations obtained on a glassy carbon electrode in 0.1 M KOH (scan rate: 200 mV s<sup>-1</sup>), (b) RDE voltammograms of 10 mM furfural at different rotation rates in 0.1 M KOH (scan rate: 50 mV s<sup>-1</sup>). (c) Levich and (d) Koutecky-Levich plots derived from Fig. 2b.

redox feature exhibited an onset potential at -1.3 V vs. Ag/ AgCl, which was independent of the substrate concentration or scan rate (ESI Fig. 7†). The cathodic maximum shifted from -1.4 V to −1.5 V vs. Ag/AgCl with increasing furfural concentration or scan rate. Cyclic voltammetry utilizing a rotating disk electrode (RDE) of carbon was employed to derive the diffusion coefficient of furfural and the electron transfer rate of its reduction. It should be noted that the background CVs of a glassy carbon electrode (GCE) in 0.1 M KOH were independent of the rotating rate (ESI Fig. 8†), illustrating that the HER was not a mass transfer-limited process within the potential window (-1.0 to -2.2 V  $\nu s$ . Ag/AgCl). Upon the addition of 10 mM furfural, further scanning to more negative potentials led to a current plateau beyond -1.4 V vs. Ag/AgCl (Fig. 2b). The current plateau also increased at a higher rotating rate, confirming that the electrochemical reduction of furfural was a fast diffusion-limited process. In addition, the starting potentials of current plateaus were negatively shifted with the increase in both electrode rotation rate and substrate concentration (ESI Fig. 9†), which could be attributed to the irreversible nature of furfural reduction in 0.1 M KOH. Based on the current plateau within -1.7 V to -2.0 V vs. Ag/AgCl, a linear relationship between the current and rotation rate was obtained, which could be fitted by a Levich plot shown in Fig. 2c. The nearly overlapped fitting curves from -1.7 V to -2.0 V vs. Ag/AgCl demonstrated a first-order reaction. The diffusion coefficient was calculated to be  $1.06 \times 10^{-5}$  cm<sup>2</sup> s<sup>-1</sup>, which was comparable to most carbohydrates in water.35 Additionally, the linear relationship between the kinetic-controlled current from -1.4 to -1.5 V vs. Ag/AgCl and the rotation rate could be fitted via the Koutecky-Levich plots (Fig. 2d), whose intercepts versus overpotential (ESI Fig. 11†) enabled the calculation of an electron transfer rate of 0.05 cm s<sup>-1</sup> (see

**Green Chemistry Paper** 

more details in the ESI†), under the assumption that the first reduction step is a one-electron process.<sup>31</sup>

Next, bulk electrolysis was carried out to probe the production of hydrofuroin from the reductive coupling of furfural. Built upon the aforementioned cyclic voltammetry studies, 100 mM furfural was reduced at -1.4 V vs. Ag/AgCl in 0.1 M KOH using a carbon paper electrode in a two-compartment batch electrolyzer. Fig. 3a and b show the current evolution and passed charge over time, respectively, during electrolysis. It was apparent that a rapid current decrease was observed within the first 5 h and accordingly the passed charge accumulated to a plateau after 5 h of electrolysis, which was due to substrate consumption. High-performance liquid chromatography (HPLC) was adopted to identify and quantify furfural and hydrofuroin based on their respective calibration curves (ESI Fig. 12†). The furfural conversion and hydrofuroin production were manifested in the evolution of HPLC traces (ESI Fig. 13†) over the passed charge. After 90 C charge was consumed, a hydrofuroin yield of ~94% was obtained together with a faradaic efficiency of 93% (Fig. 3c). Further extended electrolysis after consuming 100 C charge did not lead to higher hydrofuroin yield, whereas the faradaic efficiency slightly dipped to 88%.

Even though the above electrolysis in a batch-type electrolyzer achieved a high yield and faradaic efficiency, it inevitably required a very long time to completely convert furfural because of the extremely slow reaction rate at a low substrate concentration. With the aim of future large-scale application in mind, we next explored the practicability of flow electrolysis for furfural coupling (a flow electrolyzer schematic is shown in ESI Fig. 14†), 36,37 which was anticipated to realize constant

substrate concentration and hence maintain a high reaction rate. A two-electrode configuration was adopted, using carbon paper as the cathode and nickel foam deposited with nickel nanoparticles as the anode, which were separated by an anion exchange membrane. The appropriate voltage gap applied between the two electrodes was determined from the linear sweep voltammograms obtained in the absence and presence of 10 mM furfural in the flow electrolyte of 0.1 M KOH (ESI Fig. 15†). The much higher cathodic current between -1.6 and -2.3 V upon the addition of furfural indicated favorable furfural reduction over the HER in this voltage range. Therefore, a series of electrolysis experiments were performed at -1.9, -2.0, -2.1, -2.2, and -2.3 V. The chronoamperometry curves showed that the current remained nearly constant over time (Fig. 3d) with linearly accumulated charge (Fig. 3e) at all of these applied voltages, distinct from those in batch electrolysis (Fig. 3a and b). Outlet electrolytes were analyzed via <sup>1</sup>H NMR (ESI Fig. 16†) in real time. As plotted in Fig. 3f, the furfural conversion and hydrofuroin yield both increased when more negative voltage was applied on the working electrode, achieving over 80% yield of hydrofuroin beyond -2.1 V. Nevertheless, more negative applied voltage was also beneficial for H<sub>2</sub> evolution, which would result in a lower faradaic efficiency. For instance, even though a 94% hydrofuroin yield was obtained at -2.3 V, the corresponding faradaic efficiency was only 24%. Considering both yield and efficiency, the optimal applied voltage was -2.1 V, which resulted in a high hydrofuroin yield of 89% and an excellent faradaic efficiency of 82%. Due to the modular nature of the flow electrolyzer, it is envisioned that fine tuning the electrolysis parameters, including the electrodes (size and surface area), electrolyte,

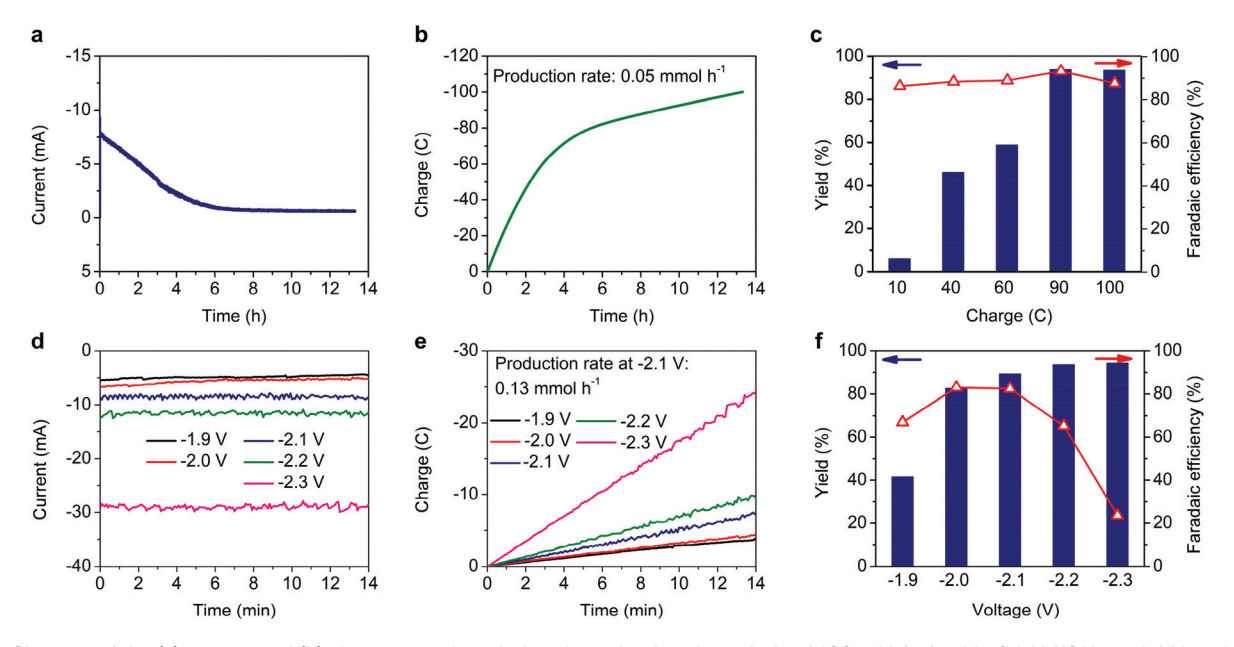


Fig. 3 Changes of the (a) current and (b) charge over time during the reductive electrolysis of 100 mM furfural in 0.1 M KOH at -1.4 V vs. Ag/AgCl. (c) Furfural conversion, hydrofuroin yield, and faradaic efficiency with different amounts of passed charge during electrolysis. Changes of the (d) current and (e) charge over time during the reductive electrolysis of 10 mM furfural in 0.1 M KOH using a two-compartment flow electrolyzer (flow rate:  $0.5 \text{ mL min}^{-1}$ ). (f) Furfural conversion, hydrofuroin yield, and faradaic efficiency at different applied potentials.

flow rate, applied voltage, membrane, compartment, *etc.*, will further improve the overall performance. Eventually, the electrochemically produced hydrofuroin can be hydrodeoxygenated following a reported route<sup>38</sup> to form  $C_{10}H_{22}$ , a linear alkane with an appropriate molecular weight in the jet fuel range  $(C_8-C_{15})$ .<sup>39</sup>

On the basis of the above experimental data, the economic advantage of our furfural upgrading approach to obtain a jet fuel precursor is roughly estimated. The average selling price of furfural in recent years is about \$1.0  $\mbox{kg}^{-1}.^{40}$  Other necessary chemical reagents such as 0.1 M KOH solution and electricity (\$0.07  $\mbox{kW}^{-1}$  h $^{-1}$ ) are much less expensive than chemicals such as ionic liquids  $^{16,17}$  used in other furfural-upgrading approaches. Given the established hydrodeoxygenation step from hydrofuroin to decane  $^{39}$  and the four times higher selling price of decane (\$4.5  $\mbox{kg}^{-1})^{41}$  relative to furfural, we are confident that our electrochemical strategy for furfural coupling bears great economic potential.

#### Conclusions

In summary, we have presented the electrohydrodimerization of furfural to generate hydrofuroin, which has an ideal carbon number (C<sub>10</sub>) to serve as a jet fuel precursor. Detailed electrochemical studies were conducted to investigate the reduction mechanism of furfural on carbon electrodes under alkaline conditions. Flow electrolysis further proved its feasibility and suitability for the practical production of hydrofuroin on a large scale. Several advantages of this electrochemical C-C coupling of furfural could be derived as listed here: (i) electroreductive coupling is performed under ambient conditions (room temperature and atmospheric pressure); (ii) water is utilized as the hydrogen source and no expensive/toxic catalysts or other chemicals are required; (iii) a high yield/selectivity of hydrofuroin is achieved together with a high faradaic efficiency; and (iv) the reaction is solely driven by electricity, which could be generated from renewable energy sources. Overall, electrochemical C-C coupling is expected to gain increasing attention not only in biomass valorization but also in more general organic synthesis.

#### Conflicts of interest

There are no conflicts to declare.

## Acknowledgements

Y. S. acknowledges the financial support from the National Science Foundation (CHE-1914546) and the University of Cincinnati. NMR experiments were performed on a Bruker AVANCE NEO 400 MHz NMR spectrometer funded by NSF-MRI grant CHE-1726092.

#### References

- 1 S. Solomon, G. K. Plattner, R. Knutti and P. Friedlingstein, *Proc. Natl. Acad. Sci. U. S. A.*, 2009, **106**, 1704–1709.
- 2 D. M. Alonso, J. Q. Bond and J. A. Dumesic, Green Chem., 2010, 12, 1493–1513.
- 3 G. W. Huber, S. Iborra and A. Corma, *Chem. Rev.*, 2006, **106**, 4044–4098.
- 4 X. Li, P. Jia and T. Wang, ACS Catal., 2016, 6, 7621-7640.
- 5 R. J. Van Putten, J. C. Van Der Waal, E. De Jong, C. B. Rasrendra, H. J. Heeres and J. G. de Vries, *Chem. Rev.*, 2013, **113**, 1499–1597.
- 6 C. H. Zhou, X. Xia, C. X. Lin, D. S. Tong and J. Beltramini, Chem. Soc. Rev., 2011, 40, 5588–5617.
- 7 H. Zang, K. Wang, M. Zhang, R. Xie, L. Wang and E. Y. X. Chen, Catal. Sci. Technol., 2018, 8, 1777–1798.
- 8 R. Mariscal, P. Maireles-Torres, M. Ojeda, I. Sádaba and M. L. Granados, *Energy Environ. Sci.*, 2016, **9**, 1144–1189.
- 9 P. Nilges and U. Schröder, Energy Environ. Sci., 2013, 6, 2925–2931.
- 10 Y. Román-Leshkov, C. J. Barrett, Z. Y. Liu and J. A. Dumesic, *Nature*, 2007, 447, 982.
- 11 T. Wang, M. W. Nolte and B. H. Shanks, *Green Chem.*, 2014, **16**, 548–572.
- 12 J. P. Lange, E. Van Der Heide, J. van Buijtenen and R. Price, *ChemSusChem*, 2012, 5, 150–166.
- 13 W. S. Lee, Z. Wang, W. Zheng, D. G. Vlachos and A. Bhan, *Catal. Sci. Technol.*, 2014, 4, 2340–2352.
- 14 M. J. Climent, A. Corma and S. Iborra, *Green Chem.*, 2014, 16, 516–547.
- 15 N. Luo, T. Montini, J. Zhang, P. Fornasiero, E. Fonda, T. Hou, W. Nie, J. Lu, J. Liu, M. Heggen, L. Lin, C. Ma, M. Wang, F. Fan, S. Jin and F. Wang, *Nat. Energy*, 2019, 4, 575–584.
- 16 L. Wang and E. Y. X. Chen, ACS Catal., 2015, 5, 6907-6917.
- 17 B. L. Wegenhart, L. Yang, S. C. Kwan, R. Harris, H. I. Kenttämaa and M. M. Abu-Omar, *ChemSusChem*, 2014, 7, 2742–2747.
- 18 F. Harnisch and U. Schröder, *ChemElectroChem*, 2019, 6, 4126–4133.
- 19 Y. Kwon, K. J. P. Schouten, J. C. van der Waal, E. de Jong and M. T. Koper, ACS Catal., 2016, 6, 6704–6717.
- 20 K. Li and Y. Sun, Chem. Eur. J., 2018, 24, 18258-18270.
- 21 L. Du, Y. Shao, J. Sun, G. Yin, C. Du and Y. Wang, *Catal. Sci. Technol.*, 2018, **8**, 3216–3232.
- 22 Y. R. Zhang, B. X. Wang, L. Qin, Q. Li and Y. M. Fan, *Green Chem.*, 2019, 21, 1108–1113.
- 23 S. Carl, K. Waldrop, P. Pintauro, L. T. Thompson and W. A. Tarpeh, *ChemElectroChem*, 2019, **6**, 5563–5570.
- 24 K. J. Carroll, T. Burger, L. Langenegger, S. Chavez, S. T. Hunt, Y. Román-Leshkov and F. R. Brushett, *ChemSusChem*, 2016, **9**, 1904–1910.
- 25 B. You, N. Jiang, X. Liu and Y. Sun, *Angew. Chem., Int. Ed.*, 2016, 55, 9913–9917.
- 26 N. Jiang, B. You, R. Boonstra, I. M. Terrero Rodriguez and Y. Sun, *ACS Energy Lett.*, 2016, 1, 386–390.

Green Chemistry Paper

- 27 B. You, X. Liu, X. Liu and Y. Sun, ACS Catal., 2017, 7, 4564–4570.
- 28 B. You, X. Liu, N. Jiang and Y. Sun, *J. Am. Chem. Soc.*, 2016, **138**, 13639–13646.
- 29 A. S. May and E. J. Biddinger, ACS Catal., 2020, 10, 3212–3221.
- 30 J. P. Stradins, *Electrochim. Acta*, 1964, **9**, 711–720.
- 31 S. Jung and E. J. Biddinger, *Energy Technol.*, 2018, **6**, 1370–1379.
- 32 X. H. Chadderdon, D. J. Chadderdon, J. E. Matthiesen, Y. Qiu, J. M. Carraher, J. P. Tessonnier and W. Li, *J. Am. Chem. Soc.*, 2017, **139**, 14120–14128.
- 33 J. C. Moutet, Org. Prep. Proced. Int., 1992, 24, 309-325.
- 34 J. Ludvík, Reduction Aldehydes Ketones, and Azomethines, in *Organic Electrochemistry*, ed. O. Hammerich and B. Speiser, CRC Press, Boca Raton, USA, 2015, pp. 1201–1247.

- 35 E. L. Cussler, *Diffusion: mass transfer in fluid systems*, Cambridge University Press, Cambridge, U.K., 2009.
- 36 M. Atobe, H. Tateno and Y. Matsumura, *Chem. Rev.*, 2017, **118**, 4541–4572.
- 37 A. A. Folgueiras-Amador and T. Wirth, *J. Flow Chem.*, 2017, 7, 94–95.
- 38 Y. B. Huang, Z. Yang, J. J. Dai, Q. X. Guo and Y. Fu, *RSC Adv.*, 2012, **2**, 11211–11214.
- 39 R. M. West, Z. Y. Liu, M. Peter and J. A. Dumesic, ChemSusChem, 2008, 1, 417–424.
- 40 A. Kuznetsov, G. Kumar, M. A. Ardagh, M. Tsapatsis, Q. Zhang and P. J. Dauenhauer, *ACS Sustainable Chem. Eng.*, 2020, **8**, 3273–3282.
- 41 H. Nezammahalleh, T. A. Adams II, F. Ghanati, M. Nosrati and S. A. Shojaosadati, *Algal Res.*, 2018, 35, 547–560.